International Journal of Applied Mathematics

Volume 38 No. 12s, 2025

ISSN: 1311-1728 (printed version); ISSN: 1314-8060 (on-line version)

MATHEMATICAL AND EXPERIMENTAL INVESTIGATION OF TAYLOR BUBBLE-INDUCED HYDROSTATIC PRESSURE REDUCTION IN NO-OVERFLOW VERTICAL TUBE

Wael Dalaf [1 2 *], Na Wei [1 2 *], Jiang Wu [1 2], Mustafa Salman [1]

[1] State Key Laboratory of Oil and Gas Reservoir Geology and Exploitation Southwest Petroleum University, Chengdu 610500, China.

[2] State Key Laboratory of Natural Gas Hydrate, Beijing 100027, China

*Corresponding authors: waeldalaf89@yahoo.com ; waelidalaf@gmail.com

Abstract

Taylor bubbles are commonly found in the petroleum, chemical, and energy industries. Typically, a Taylor bubble decreases hydrostatic pressure due to its lower density than the surrounding fluid. However, this study identifies an additional mechanism for Taylor bubble contributing to hydrostatic pressure reduction. This effect arises from the dynamic upward motion of the Taylor bubble, where the bubble tends to push the surrounding liquid upward, depending on its buoyancy. An experiment was conducted in which a single Taylor bubble was injected into a vertical tube. A pressure drop from 6500 Pa to 6370 Pa and from 6500 Pa to 6141 Pa was observed when injecting 3 mL and 13 mL of Taylor bubble volume, respectively. The rise speed and diameter of the Taylor bubble, as well as the speed and thickness of the liquid film around it, were measured using a pulse-echo ultrasonic technique. The ultrasonic measurements showed that instantaneous upward and downward flow rates were not equal. The upward flow rate was dominant, which caused a drop in pressure at the bottom of the tube. Finally, these findings can help these industries to predict the bottom hole or pipe pressure accurately.

Keywords: Taylor bubble; Liquid film; Bernoulli's principle; Archimedes' Principle; Hydrostatic Pressure; Fluid.

Introduction

Taylor bubbles are very significant in petroleum and chemical engineering applications, such as gas kicks during drilling, gas-lift oil production, heat exchangers, and many other energy applications. In this study, we experimentally demonstrate that the Taylor bubble plays a second role in reducing hydrostatic pressure by pushing the fluid upward as it rises, in addition to its primary role in reducing hydrostatic pressure due to its low density relative to the surrounding liquid, a phenomenon not previously reported.

In 1950, Taylor investigated the so-called Taylor bubble [1] , with particular emphasis on its shape and rise velocity, and showed experimentally that the rise velocity increases with increasing the diameter of the pipe. Earlier, in 1943, Dumitrescu had examined the same class of long gas bubbles [2] , analyzing their shape and rise velocity in vertical tubes. By applying Bernoulli's principle, Dumitrescu derived an expression for the rise velocity and indicated the role of the bubble in generating fluctuations in the surrounding dynamic pressure. Neither

Volume 38 No. 12s, 2025
ISSN: 1311-1728 (printed version); ISSN: 1314-8060 (on-line version)

Taylor nor Dumitrescu, however, explicitly addressed the role of the Taylor bubble in reducing the hydrostatic pressure. Although both authors obtained the same functional form for the Taylor-bubble rise velocity, they reported slightly different values of the proportionality constant, as expressed in the following relation.

$$VTb = FrTb \times \sqrt{g \times DTube}$$

where V_{Tb} is the Taylor bubble velocity, Fr_{Tb} is the Taylor bubble froude number, g is the gravitational acceleration, D is the pipe diameter.

This paper explains how Taylor bubbles can lower the hydrostatic pressure in a vertical pipe without fluid overflow. The motion of the bubble can be viewed as an application of Bernoulli's principle in fluid mechanics. Every Taylor bubble that goes into the pipe pushes the fluid up. This makes the fluid column at the bottom of the tube seem lighter, which shows up as a drop in pressure. Table 1 shows the experimental data that explains this effect in numbers. According to Archimedes' principle, buoyancy increases as the volume of the submerged object increases. [3] [4] , following the relationship below.

$Fbnt = \rho water \times volTb \times g$

where F_{bnt} is the buoyant force, vol_{Tb} is the Taylor bubble volume, g is the gravitational acceleration.

The balance between the object's weight and buoyant force controls how it moves while it is submerged. It will move down if its weight is greater than the buoyant force. The body is in static equilibrium when the two forces are equal. In contrast, if the buoyant force is stronger than the weight, the object moves up [5] [6] . Gawusu showed that the pressure dropped surrounding the Taylor bubble as it rose in the tube [7] . Klaseboer et al. also mentioned that the pressure dropped behind the Taylor bubble [8] . But in our study, we discovered that the pressure decrease was the same along the whole length of the liquid column until the Taylor bubble went out of the water column. The main forces that control the movement of gas bubbles that are underwater are gravity, buoyancy, and drag. For large bubbles, like ascending Taylor bubbles, the buoyant force is usually stronger than the total of the drag and gravity forces. This makes them move up continuously. As the size of the bubble increases, the buoyant force increases significantly. This raises the net driving force and speeds up the bubble's rise [9] [10].

As the tube's diameter gets smaller or the reverse flow of liquid from top to bottom gets stronger, the frictional force on the bubble gets stronger. This eventually causes the bubble to reach dynamic equilibrium or stop moving in the tube [11] [12] . As the viscosity of the fluid around the Taylor bubble increases, the frictional forces acting on it get stronger, which slows down its ascent speed by a lot [13] . [14] refers to the shear rate that the bubble's rise caused in the liquid next to it.

When a Taylor bubble rises in a vertical pipe without causing the gasliquid system to overflow, the hydrostatic pressure drops because of the complex interplay between the bubble's dynamic properties and the pipe's dynamic properties. From an energy point of view, the liquid film that is going down meets friction at two places: one with the pipe wall and the other with the Taylor

Received: August 06, 2025

bubble interface. The Taylor bubble, on the other hand, only has friction when it touches the liquid sheet. This asymmetry causes more energy to flow up than down, which leads to the net energy loss that may be seen as a drop in pressure [15].

In fact, this phenomenon is consistent with Bernoulli's principle, which states that an increase in velocity causes a decrease in hydrostatic pressure. Initially, the water column was stationary in the experiment, and the pressure was constant. However, as soon as the Taylor bubble entered, it locally increased the velocity of the liquid, leading to a pressure drop. The rise of the Taylor bubble is indeed an example of an application of this principle, and it bears some similarity to air jets in water conduits, but at a much lower speed [16] [17] [18] . This study will enhance well-control safety and improve the accuracy of predicting total hydrostatic pressure, either in gas-lift oil production or in a vertical multiphase flow system.

2 Materials and Methods

2.1 Experimental Apparatus

A-An experimental setup was constructed, including several components. First, a graduated transparent acrylic tube (length 1.0 m, inner diameter 1 cm) was used for visual observation. Second, water at 20˚C, with density ρ = 1000kg/m^3, dynamic viscosity $\mu = 1.0 \times 10^{-3}$ Pas, and surface tension σ = 0.0728N/m, was filled to a height of 0.663 m above the level of the pressure gauge.. Third, a non-return valve was placed between the air syringe and the acrylic tube to prevent water backflow and resulting loss of air pressure after the Taylor bubble was injected. Fourth, an air syringe supplied air at a density of 1.225 kg/m‡ to generate Taylor bubbles. The setup also included an electronic pressure gauge (SEH-type), which measured pressure with Pascal-level accuracy, –2 Pa. The entire setup with its dimensions is shown in **Figure 1**

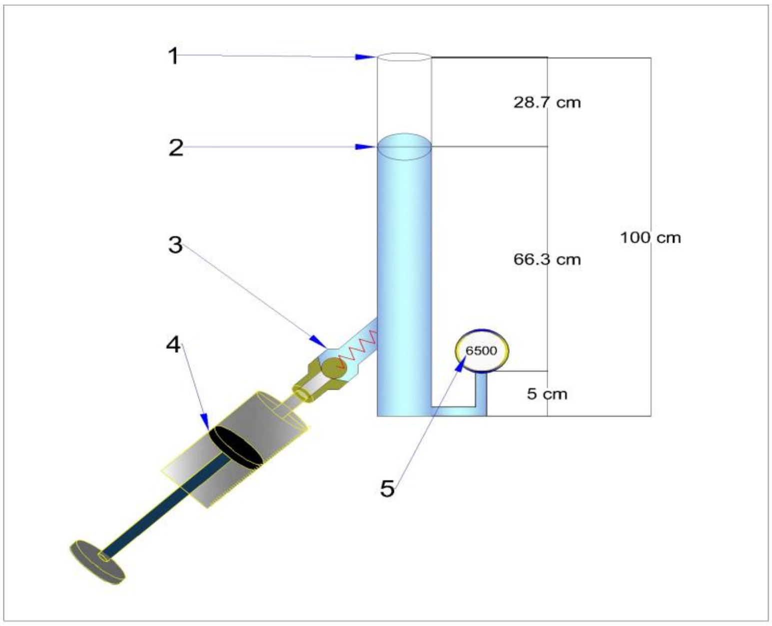

Figure 1: Experimental setup diagram before bubble injection: (1) acrylic tube, (2) water column, (3) non-return valve, (4) air syringe, (5) electronic pressure gauge.

International Journal of Applied Mathematics
Volume 38 No. 12s, 2025
ISSN: 1311-1728 (printed version); ISSN: 1314-8060 (on-line version)

B-Additionally, a pulse-echo ultrasonic system was installed along the acrylic tube to measure the rise velocity of the Taylor bubble, the downward velocity of the liquid film, and the dimensions of both the bubble and the liquid film.

2.2 Experimental Procedure

The experiment was conducted at atmospheric pressure with a temperature of 20 degrees Celsius.

1. The density of the water was measured and found to be 1000 kg/m‡. 2. The acrylic tube was filled with water to a height of 66.3 cm, leaving an air gap at the top of length 28.7 cm (0.287 m), to prevent overflow during air injection 3. The system was left for one minute to ensure pressure stabilized at the initial hydrostatic pressure of 6500 Pa, verified by gauge readings. 4. A single Taylor bubble (volume: 3 mL) was injected into the tube without causing overflow. During the bubble passage, the hydrostatic pressure dropped from 6500 Pa to 6370 Pa and returned to its initial value upon exiting the column. 5. Step 4 was repeated for various injected air volumes for three runs, generating Taylor bubbles of different sizes, with all measurements performed under no-overflow conditions. Increased injected volumes consistently resulted in greater observed pressure drops **(see Figure 2 and Table 1).**

6. To find the Taylor bubble rise velocity, the liquid film thickness, the bubble diameter, and the film development length, a pulse-echo ultrasonic technique was used. Because the gas and liquid phases have very different acoustic impedances, almost all of the ultrasonic wave is reflected at the gas–liquid interface. When the Taylor bubble moves in front of the ultrasonic system, short ultrasonic pulses are sent out and bounced back from the bubble's nose and the liquid film around it. The time-of-flight method is used to turn the returned echoes into electrical signals and figure out the thickness of the bubble and the liquid film. The Doppler frequency shifts in the reflected signals are then used to figure out how fast the Taylor bubble is rising and how fast the liquid film is falling.

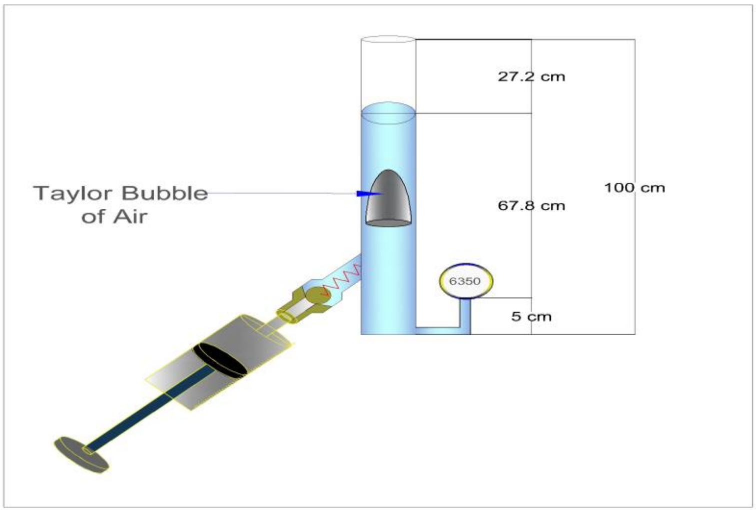

Figure 2: Rising Taylor bubble with a volume of 3 mL without water overflow induced a hydrostatic pressure drop from 6500 Pa to 6370 Pa during its ascent.

Received: August 06, 2025

International Journal of Applied Mathematics
Volume 38 No. 12s, 2025
ISSN: 1311-1728 (printed version); ISSN: 1314-8060 (on-line version)

3Mathematical Model of Pressure Drop

3.1 Assumptions

1. Given that the hydrostatic pressure above the Taylor bubble is very lowand that the effect of air compressibility under these conditions is negligible, it was assumed in this study that the injected air volume is equal to the volume of the Taylor bubble formed inside the tube.

2. Since the weight of the Taylor bubble is negligibly small comparedwith the friction and buoyancy forces acting during its rise in the tube, the effect of the bubble weight was neglected in the analysis. Accordingly, the analytical model considers only two opposing forces: the upward buoyancy force and the downward frictional force

3.2 Buoyant Force (F_{bnt})

The buoyancy force depends on both the surrounding fluid density and the submerged object volume. Theoretically, it can be calculated according to Archimedes' principle.

$$Fbnt = \rho water \times VolTb \times g \qquad (1)$$

3.3 Geometrical Description

3.3.1 Tube Area (A_{Tube})

The cross-sectional area of the tube can be determined by the following equation

$$A_{Tube} = \pi \times (\frac{D_{Tube}}{2})^2 \qquad (2)$$

where A_{Tube} is the Tube cross-sectional area, D_{tube} is the Tube diameter.

3.3.2 Taylor Bubble Area (A_{Tb})

After determining the diameter of the Taylor bubble using the pulse-echo ultrasonic system, the cross-sectional area of the bubble can be calculated using the following equation:

$$A_{Tb} = \pi \times (\frac{D_{Tb}}{2})^2 \qquad (3)$$

where A_{Tb} is the Taylor bubble cross-sectional area, D_{Tb} is the Taylor bubble diameter.

3.3.3 Liquid Film Area (A_{Lf})

After the film thickness was measured using the pulse-echo ultrasonic system, the liquid film area can be calculated using the following equation:

$$A_{Lf} = \pi \times (2 \times R_{Tube} \times \delta - \delta^2) \approx 2 \times \pi \times R_{Tube} \times \delta \qquad (4)$$

Or can be obtained by subtracting the Taylor bubble cross-sectional area from the tube cross-sectional area as shown:

$$ALf = ATube - ATb \qquad (5)$$

where A_{Lf} is the Liquid film cross-sectional area, δ is the Liquid film thickness.

Received: August 06, 2025

ISSN: 1311-1728 (printed version); ISSN: 1314-8060 (on-line version)

3.4Theoretical Liquid Film Thickness (δ)

The liquid film thickness can be calculated mathematically using any of the following relationships.

3.4.1Taylor Bubble Reynolds Number (Re_{Tb})

The Taylor bubble Reynolds number is defined as [19] :

$$Re_{Tb} = \frac{\rho_{water} \times V_{Tb} \times D_{Tube}}{\mu_{water}} \quad (6)$$

Where Re_{Tb} is Taylor bubble Reynolds Number, V_{Tb} is the Taylor bubble velocity, μ_{water} is the water viscosity.

3.4.2Dimensionless Inverse Viscosity Number (N_f)

By combining the Eötvös number and the Morton number, the dimensionless inverse viscosity number can be obtained [20] [21].

$$N_f = \left(\frac{Eo^3}{M}\right)^{0.25} = (\frac{\rho_{water}}{\mu_{water}}) \times \sqrt{g \times D^3_{Tube}} \quad (7)$$

2

Where Eo is the E¨otvo¨s number ($\frac{\rho_{water} \times g \times ^{D_{Tube}}}{\sigma_{water}}$) , M is the Morton number ($\frac{g \times \mu^4_{water}}{\rho_{water} \times \sigma^3_{water}}$), σ_{water} is the water surface tension.

3.4.3 Nusselt Correlation (δ'_{ns})

$$\delta'_{ns} = \left(6 \times \frac{Re_{Tb}}{N_f^2}\right)^{1/3} \quad (8)$$

Where δ'_{ns} is the dimensionless liquid film thickness predicted by Nusselt[22]. **3.4.4 Karapantsios and Karabelas correlation (δ'_{kar})**

$$\delta'_{kr} = \frac{0.428 \times Re_{Tb}^{0.538}}{\sqrt[3]{N_f^2}} \quad (9)$$

Where δ_{kr}' is the dimensionless liquid film thickness obtained from the correlation of Karapantsios and Karabelas [23].

3.4.5 Lel et al.b (δ'_{le})

$$\delta'_{le} = \frac{2 + 0.641 \times Re_{Tb}^{0.47}}{\sqrt[3]{N_f^2}} \quad (10)$$

Where δ'_{le} is the dimensionless liquid film thickness obtained from the correlation of Lel et al. [24] .

3.4.6Dimensional and Dimensionless Liquid Film Thickness

The correlations shown above predict the dimensionless liquid film thickness δ'. To compare it directly with experimental measurements, it needs to be changed into the dimensional film thickness by incorporating δ' with the tube radius R_{Tube}, as shown below:

$$\delta = \delta' \times RTube \qquad (11)$$

3.5Upward and Downward Flow Rate (Q_{Tb})

3.5.1Taylor Bubble Flow Rate (Q_{Tb})

Using the Pulse-Echo Ultrasonic System, a very slight increase in the upward velocity of the Taylor bubble was observed. This velocity is proportional to the size of the Taylor bubble, as shown in Table 2. This behavior is expected because the larger bubble rises faster than the smaller one, and the slight increase in the Taylor bubble's velocity cannot be ignored. Mathematically, the Taylor bubble flux is calculated using the following equation.

$$QTb = ATb \times VTb \qquad (12)$$

where Q_{Tb} is the upward water flow rate induced by Taylor bubble, V_{Tb} is the Taylor bubble velocity

3.5.2 Liquid Film Flow Rate (Q_{Lf})

It was also observed that there was a slight increase in the liquid film velocity determined by the Pulse-Echo Ultrasonic System, as shown in the table 3, which is directly proportional to the size of the Taylor bubble. However, the flow rate of increase by the liquid film is less than the rate of increase in the Taylor bubble. The important point we want to emphasize is that the liquid film around the Taylor bubble does not fall solely due to gravity but also due to the suction effect induced by the high velocity below the Taylor bubble.

Therefore, the liquid film falls at a very high velocity. Mathematically, the flow rate of the liquid film is calculated using the following equation.

$$QLf = ALf \times VLf \qquad (13)$$

where Q_{Lf} is the downward water flow rate of the liquid film, V_{Lf} is the velocity of the falling liquid film.

3.6 Bottom Pressure (P)

3.6.1 Static Pressure (P_0)

The pressure in this case is the hydrostatic pressure at the bottom of the tube under static conditions, prior to the injection of the Taylor bubble. The measured values show excellent agreement with the theoretical predictions. This pressure can be calculated using the following formula:

$$P0 = \rho water \times hwater \times g \qquad (14)$$

ISSN: 1311-1728 (printed version); ISSN: 1314-8060 (on-line version)

Where P_0 is the static pressure, ρ_{water} is the water density, h_{water} is the height of the water in the tube, g is the gravitational acceleration.

3.6.2Transient Bottom Pressure (P_{tr})

When a Taylor bubble is injected into the tube, the pressure around the bubble changes in a small area, which directly affects the bottom pressure. As the bubble rises, it induces an upward motion of the liquid, while a downward flow simultaneously forms along the thin liquid film surrounding it. Because these two opposing flows do not establish instantaneously and differ slightly in magnitude, a temporary imbalance arises. This imbalance results in a transient pressure drop at the bottom of the tube, as the pressure gauge does not instantaneously sense the entire water column, even though no liquid escapes the system. Consequently, the bottom pressure during this transient phase can be described mathematically by the following relationships.

$$K = \frac{Q_{Downward}}{Q_{Upward}}$$

or

$$K = \frac{Q_{Lf}}{Q_{Tb}} \qquad (15)$$

Where K is the instantaneous counter-flow imbalance coefficient. This coefficient describes the transient bottom pressure, which can be represented by the following equation.

$$Ptr = K \times P0 \qquad (16)$$

If $Qupward = Qdownward,$ $\quad K = 1 \quad Ptr = P0$

If $Qupward > Qdownward,$ $\quad K < 1 \quad Ptr < P0$

where P_{tr} is the transient bottom pressure

4 Result

Table 1: Measured hydrostatic pressure response to the injected volume of single Taylor bubbles of air, with three repeats for each volume.

N	Vol_{Tb} (mL)	L_{Tb} (cm)	P_m (Pa)			Average P_m (Pa)
			Run 1	Run 2	Run 3	
1	0	0	6500	6500	6500	6500
2	3	4.6	6370	6372	6366	6370
3	4	6.1	6344	6348	6347	6347
4	5	7.6	6326	6324	6324	6325
5	6	9.2	6299	6297	6299	6298

International Journal of Applied Mathematics
Volume 38 No. 12s, 2025
ISSN: 1311-1728 (printed version); ISSN: 1314-8060 (on-line version)

6	7	10.7	6283	6277	6276	6279
7	8	12.2	6258	6259	6256	6258
8	9	13.8	6233	6232	6233	6233
9	10	15.3	6208	6211	6213	6211
10	11	16.9	6188	6190	6191	6190
11	12	18.4	6165	6163	6163	6164
12	13	19.9	6144	6140	6140	6141

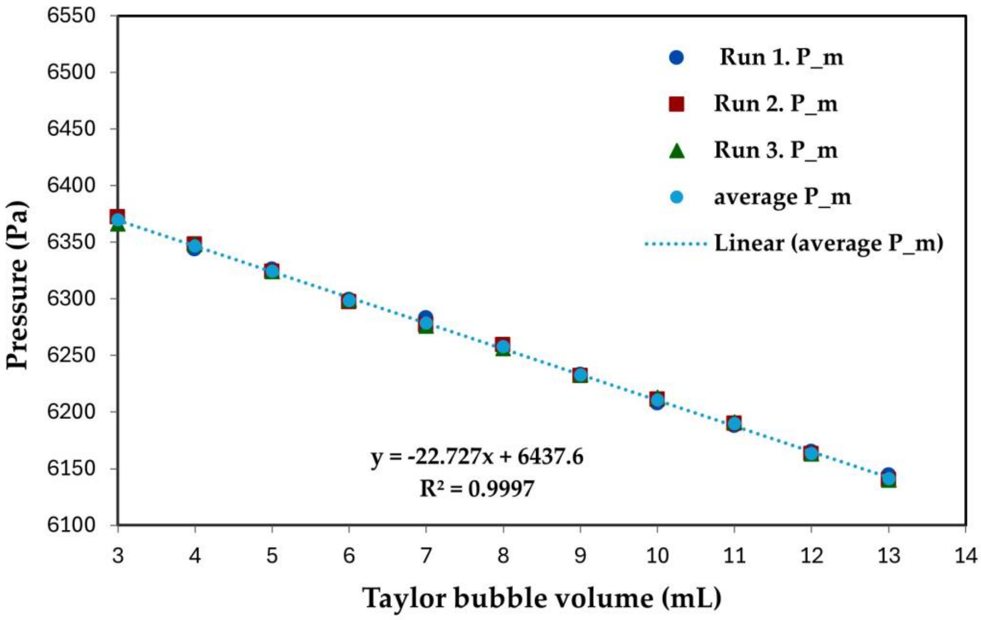

Figure 3: The average hydrostatic measured pressure from the three tests, with an R-squared value of 0.9997

Figure 3 shows a strong negative linear relationship between the volume of the injected Taylor bubble and the hydrostatic pressure measured in the tube. Every point on the graph denotes the average pressure collected from three different trials, demonstrating minimal standard deviation and narrow error bars, therefore indicating that the data is highly exact and reproducible. These results demonstrate the function of the Taylor bubble in mechanically decreasing hydrostatic pressure, rather than solely through reduced density.

Table 2: Measured diameters of the Taylor bubble and liquid film using the pulse-echo ultrasonic system

Vol_{Tb} (mL)	D_{Tb} (m)			δ (m)		
	Run 1	Run 2	Run 3	Run 1	Run 2	Run 3

Volume 38 No. 12s, 2025
ISSN: 1311-1728 (printed version); ISSN: 1314-8060 (on-line version)

0	–	–	–	–	–	–
3	0.00913	0.00913	0.00913	0.00043	0.000434	0.000436
4	0.00913	0.00913	0.00913	0.000435	0.000437	0.000436
5	0.00913	0.00912	0.00913	0.000437	0.000438	0.000436
6	0.00912	0.00912	0.00913	0.000438	0.000438	0.000437
7	0.00912	0.00912	0.00912	0.000439	0.000439	0.000438
8	0.00912	0.00912	0.00912	0.000440	0.000439	0.000440
9	0.00912	0.00912	0.00912	0.000440	0.000441	0.000441
10	0.00911	0.00912	0.00912	0.000443	0.000442	0.000441
11	0.00911	0.00911	0.00911	0.000443	0.000443	0.000443
12	0.00911	0.00911	0.00911	0.000444	0.000443	0.000444
13	0.00911	0.00911	0.00911	0.000445	0.000446	0.000444

Table 3: Average velocities of the Taylor bubble and liquid film measured using the ultrasonic system

Vol_{Tb} (mL)	v_{Tb} (m/s)			v_{Lf} (m/s)		
	Run 1	Run 2	Run 3	Run 1	Run 2	Run 3
3	0.1075	0.1076	0.1076	0.5281	0.5280	0.5287
4	0.1084	0.1086	0.1084	0.5297	0.5293	0.5296
5	0.1096	0.1093	0.1094	0.5307	0.5308	0.5301
6	0.1105	0.1104	0.1101	0.5319	0.5311	0.5318
7	0.1111	0.1112	0.1114	0.5323	0.5324	0.5330
8	0.1121	0.1122	0.1120	0.5339	0.5335	0.5333
9	0.1131	0.1132	0.1128	0.5348	0.5345	0.5343
10	0.1141	0.1141	0.1136	0.5353	0.5356	0.5354
11	0.1149	0.1149	0.1146	0.5365	0.5364	0.5361
12	0.1158	0.1158	0.1155	0.5373	0.5373	0.5370
13	0.1167	0.1167	0.1165	0.5384	0.5379	0.5378

Received: August 06, 2025

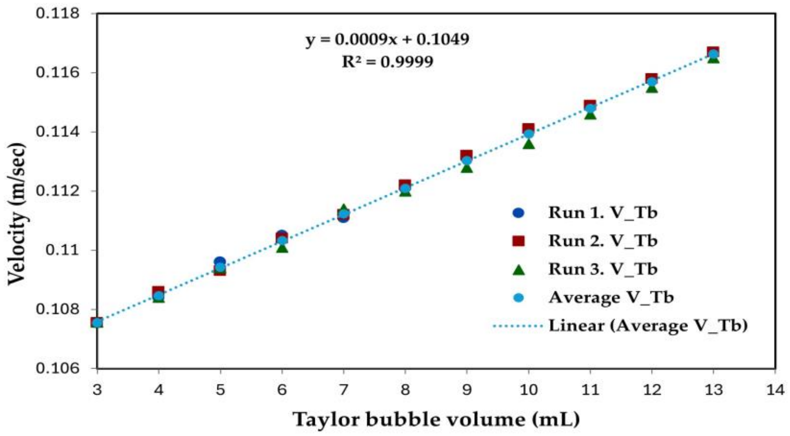

Figure 4: The slight increase in Taylor's bubble velocity recorded by the pulse-echo ultrasonic system versus the increase in bubble size (buoyancy).

Although Taylor and Dumitrescu used the same formula to determine the rising velocity of a Taylor bubble in a tube, their assumptions about the Froude number were different. Dumitrescu used a value of 0.351, while Taylor chose 0.328. The proper value of the Froude number has been the subject of much discussion among researchers as a result of this disparity. Further research has demonstrated that the Froude number is dependent on the buoyancy force acting on the bubble rather than being a universal constant. A higher rising velocity is the outcome of the Froude number increasing in proportion to the buoyancy force. However, the buoyancydriven acceleration stops when the Taylor bubble reaches its terminal (final) rising velocity, and the Froude number reaches a fixed value that corresponds to this steady-state regime [25]. Ultrasound measurements have shown a slight variation in the rising velocity of a Taylor bubble, directly proportional to its size, despite constant tube diameter. This is logical because the rising velocity of a larger bubble exceeds that of a smaller bubble due to their differing buoyancy forces.

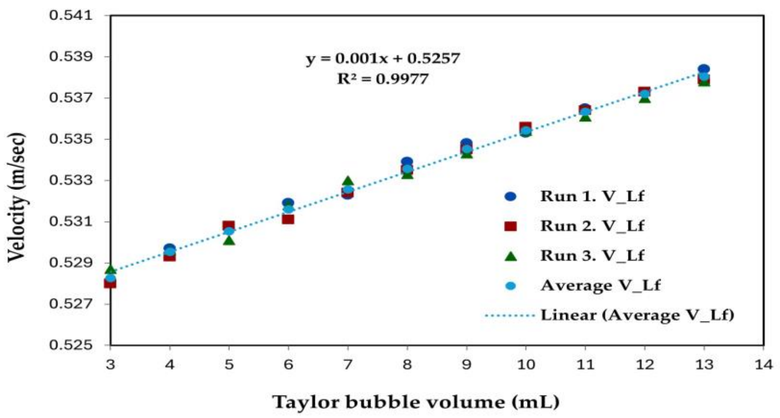

Figure 5: The slight increase in falling liquid film velocity recorded by the pulse-echo ultrasonic system versus the increase in bubble size.

International Journal of Applied Mathematics
Volume 38 No. 12s, 2025
ISSN: 1311-1728 (printed version); ISSN: 1314-8060 (on-line version)

The liquid-film velocity depends on both gravity and the suction effect induced by the Taylor bubble below it. Therefore, as the Taylor bubble increases in size, its buoyancy increases, and its speed increases, thus increasing the suction effect below the bubble. The liquid film then falls at a high speed to compensate for this decrease in volume beneath the rising Taylor bubble.

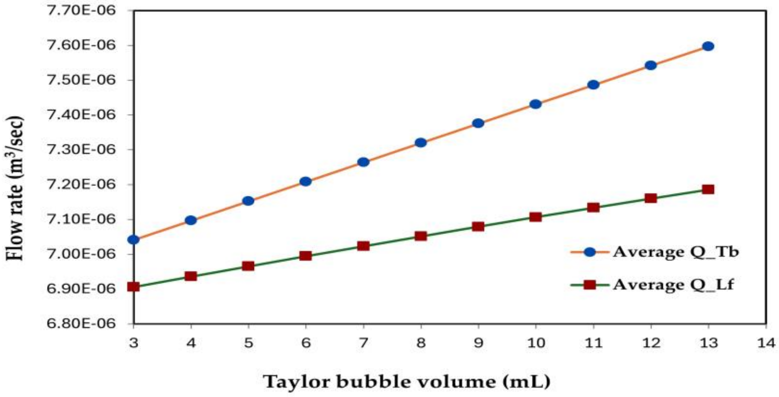

Figure 6: shows the difference between the upward water flow rate (Taylor bubble flow rate) and the downward water flow rate (liquid film flow rate)

The upward water flow rate induced by a Taylor bubble is greater than the downward flow rate of the liquid film falling around it. This occurs because the bubble experiences friction only at the liquid-film interface, whereas the liquid film experiences friction at both the tube wall and Taylor bubble interfaces. Therefore, there is a decrease in volume compensation below the rising Taylor bubble, which manifests as a pressure drop, i.e., the suction effect is evident.

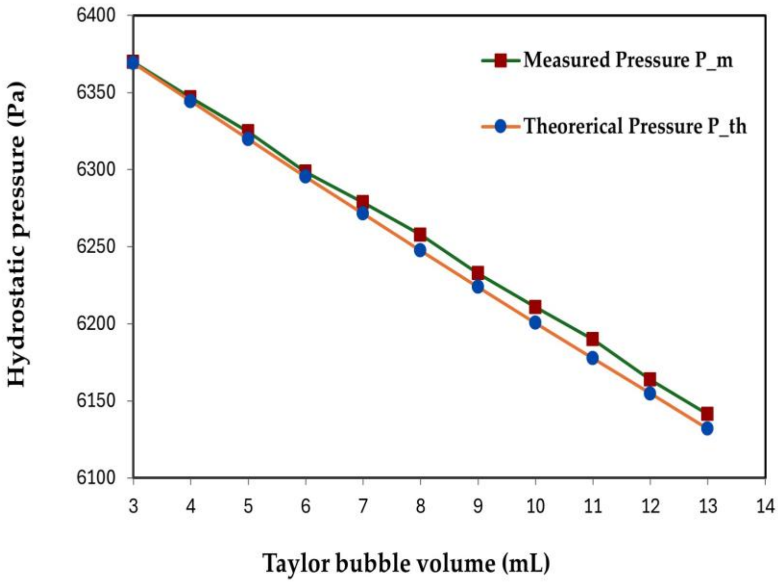

Figure 7: Convergence between the measured and theoretical hydrostatic pressures

International Journal of Applied Mathematics
Volume 38 No. 12s, 2025
ISSN: 1311-1728 (printed version); ISSN: 1314-8060 (on-line version)

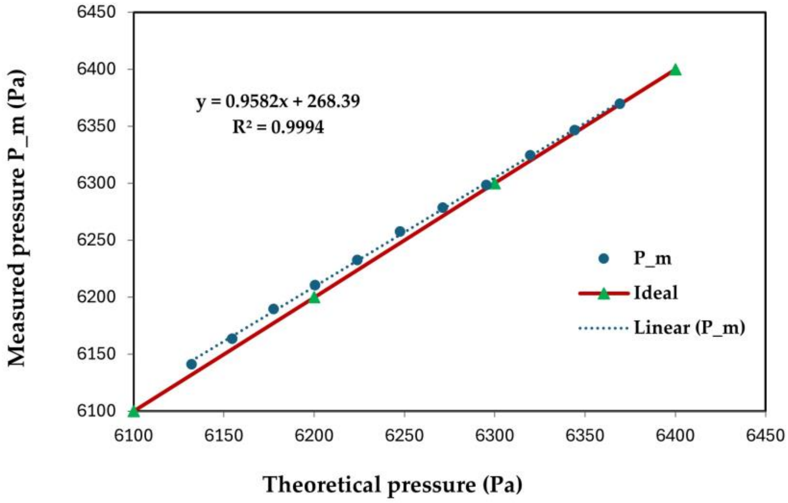

Figure 8: Convergence between measured and theoretical hydrostatic pressures (Regression = 99.94)

Figures 7 and **Figure 8** These results show that experimental and theoretical hydrostatic pressure values are very close to each other, with an agreement of about 99.9%. This shows that the model is reliable and that the measurements can be repeated very well.

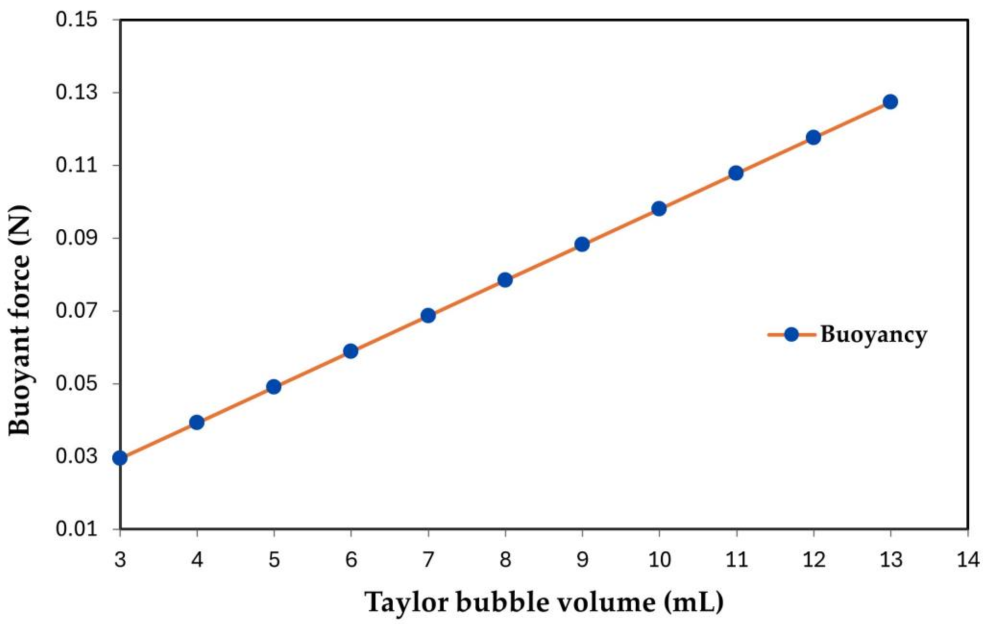

Figure 9: The buoyant force rises in a straight line as the volume of the Taylor bubble rises, showing a strong positive connection over the range (3–13 mL).

Figure 9 shows the upward buoyant force created by the Taylor bubble. This force increases almost linearly with bubble volume between 3 and 13 mL, which means that a larger volume of air displaced in the tube means a stronger buoyant force. This behavior shows that making

International Journal of Applied Mathematics
Volume 38 No. 12s, 2025
ISSN: 1311-1728 (printed version); ISSN: 1314-8060 (on-line version)

the Taylor bubble bigger makes it better at moving and raising the water, which lowers the hydrostatic pressure.

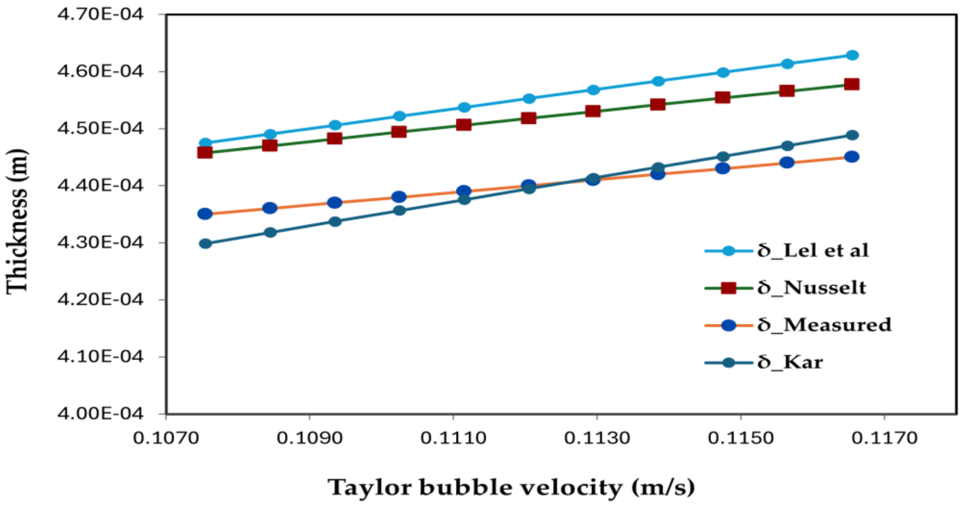

Figure 10: A comparison of the measured liquid film thickness with classical theoretical correlations (Nusselt, Karapantsios–Karabelas, and Lel et al.)

Figure 10 shows that the thickness of the liquid film increases steadily as the Taylor bubble's ascending velocity increases, as shown by ultrasonic system. To get this upward acceleration, the bubble tends to pull away from the wall of the tube, which makes the liquid film around it thicker. The experimental values for film thickness lie between the predictions of the Nusselt and Karapantsios–Karabelas relationships, whereas the Lel et al. relationship tends to overestimate the thickness within the examined velocity range.

5 Discussion

Bigger Taylor bubbles have a stronger upward driving force because they have a stronger buoyant force. This means they rise faster. Along with this rise in speed, the bubble's cross-sectional area gets a little smaller. At the same time, the liquid film around it gets thicker and moves faster. But even with these changes, the fast-rising Taylor bubble still causes more water to flow up than down through the liquid film.

This behavior aligns with classical observations documented by He [26], who indicated that the measured ascent velocity of elongated Taylor bubbles surpasses the Davies–Taylor prediction by approximately 10%. Moreover, longer Taylor bubbles demonstrate increased buoyancy, resulting in elevated Froude numbers, as indicated by Zhou and Prosperetti [27]. This phenomenon elucidates the observed rise in the Froude number in correlation with the Archimedes number within a buoyancy-dominated regime.

6 Conclusion

The mathematical model and experimental data demonstrate that the Taylor bubble works mechanically to lower hydrostatic pressure. This effect gets stronger as the volume of the

Received: August 06, 2025

Taylor bubble increases, because a larger volume creates a stronger buoyant force that allows the bubble to move and rise more easily. According to Bernoulli's principle, this happens because the fluid's speed increases, which lowers the pressure. At first, the water column and hydrostatic pressure stayed the same. But after the Taylor bubble entered the water column, the water speed changed. This study shows that the quick spread of kicks in drilling operations and the success of gas-lift production can be partially explained by how the Taylor bubble works mechanically. It lowers hydrostatic pressure and pushes the liquid up.

7 Recommendation

1. It is recommended to conduct further experiments using different pipe diameters, based on the experiment in this study, to investigate the effect of Taylor bubble size on the reduction of hydrostatic pressure, ensuring that no water is displaced outside the system during the experiments. 2. It is recommended to investigate the effect of injecting multiple Taylor bubbles through the pipe in order to assess the cumulative reduction in hydrostatic pressure caused by the presence of several bubbles, and to compare this with the single-bubble case. During such experiments, it is important to ensure that no water escapes from the pipe.

Acknowledgments: The authors would like to express their sincere gratitude to the funding agencies for their generous financial support of this research. This work was supported by the National Key Research and Development Program of China (Grant Nos. 2023YFC2811002 and 2021YFC2800903), the Director Fund Project (2025) of the State Key Laboratory of Marine Natural Gas Hydrates (Grant No. CCL2024RCPS0275KQN), the 111 Project (Grant No. D21025), and the National Natural Science Foundation of China (NSFC) (Grant No. U2444216).

References

[1] R. M. Davies and G. I. Taylor. The mechanics of large bubbles rising through extended liquids and through liquids in tubes. *Proceedings of the Royal Society of London. Series A, Mathematical and Physical Sciences*, 200(1062):375–390, February 1950.

[2] D. T. Dumitrescu. Str¨omung an einer luftblase im senkrechten rohr. *ZAMM - Zeitschrift fu¨r Angewandte Mathematik und Mechanik*, 23(3):139–149, January 1943.

[3] L. Neri et al. Enhancing buoyant force learning through a visuo-haptic environment: a case study. *Frontiers in Robotics and AI*, 11, July 2024.

[4] J. Kriek and A. Legesse. The effects of the multiple representation approach on undergraduate students' understanding of archimedes principle. *Journal of Pedagogical Research*, November 2023.

[5] K. Dunnett and A. Mattias Lundmark. The complexities of moving topics between disciplines: the case of buoyancy and isostasy. *International Journal of Science Education*, 46(12):1239–1255, August 2024.

Volume 38 No. 12s, 2025
ISSN: 1311-1728 (printed version); ISSN: 1314-8060 (on-line version)

[6] F.-J. Castillo-Hern´andez, M.-R. Jim´enez-Liso, D. Couso, and R. Lo´pezGay. Exploring the phenomena of floating and sinking in science education literature: a systematic review. *Studies in Science Education*, pages 1–30, February 2025.

[7] S. Gawusu and X. Zhang. Hydrodynamics analysis of taylor flow in oil and gas pipelines under constant heat flux. *Heat and Mass Transfer*, 57(3):515–527, March 2021.

[8] E. Klaseboer, R. Gupta, and R. Manica. An extended bretherton model for long taylor bubbles at moderate capillary numbers. *Physics of Fluids*, 26(3), March 2014.

[9] A. A. Kendoush. The drag forces on a taylor bubble rising steadily in vertical pipes. *Journal of Energy and Power Technology*, 3(4):1–13, December 2021.

[10] X. Wang, J. Zhang, Y. Chen, and Z. Kuai. Numerical study of rising taylor bubbles driven by buoyancy and additional pressure. *International Journal of Multiphase Flow*, 159:104309, February 2023.

[11] R. Maestri et al. Equilibrium taylor bubble in a narrow vertical tube with constriction. *Physics of Fluids*, 36(3), March 2024.

[12] J. Kren et al. Dynamics of taylor bubble interface in vertical turbulent counter-current flow. *International Journal of Multiphase Flow*, 165:104482, August 2023.

[13] P. Priyanka, G. Das, S. Ray, M. Kaushal, and D. Sarker. Anomalous behavior of taylor bubble rise in glycerol solutions–mechanistic insights and numerical simulations. *Physics of Fluids*, 37(7), July 2025.

[14] K. Ezeji and J. Tihon. Near-wall flow response to large air bubbles rising in inclined water channels. *Chemical Engineering Science*, 247:116914, January 2022.

[15] G. Zhou and A. Prosperetti. Faster taylor bubbles. *Journal of Fluid Mechanics*, 920:R2, August 2021.

[16] J. Ren et al. Pressure characteristics in an airlift pump system. *Physics of Fluids*, 37(2), February 2025.

[17] J. Zhu et al. Frictional pressure drop of the vertically upward gas–liquid two-phase flow in an airlift pump system. *Physics of Fluids*, 36(9), September 2024.

[18] L. Guo, H. Cheng, Z. Yao, C. Rong, J. Lin, and X. Wang. Mathematical model of velocity and distribution law in gas lift reverse circulation well washing flow field for drilling shaft sinking. *Scientific Reports*, 14(1):27327, November 2024.

[19] Christophe Clanet, Pierre H´eraud, and Geoffrey Searby. On the motion of bubbles in vertical tubes of arbitrary cross-sections: some complements to the dumitrescu–taylor problem. *Journal of Fluid Mechanics*, 519:359–376, 2004.

[20] Graham B. Wallis. *One-Dimensional Two-Phase Flow*. McGraw-Hill, New York, 1969.

Received: August 06, 2025

International Journal of Applied Mathematics
Volume 38 No. 12s, 2025
ISSN: 1311-1728 (printed version); ISSN: 1314-8060 (on-line version)

[21] Edward W. Llewellin, Enrico Del Bello, Jacopo Taddeucci, Piergiorgio Scarlato, and Stephen J. Lane. The thickness of the falling film of liquid around a taylor bubble. *Proceedings of the Royal Society A: Mathematical, Physical and Engineering Sciences*, 468:1041–1064, 2012.

[22] Wilhelm Nusselt. Die oberfl¨achenkondensation des wasserdampfes. *Zeitschrift des Vereines Deutscher Ingenieure*, 60:541–546, 1916.

[23] Theodoros D. Karapantsios and Alexandros J. Karabelas. Longitudinal characteristics of wavy falling films. *International Journal of Multiphase Flow*, 21:119–127, 1995.

[24] Vladimir V. Lel, Farouk Al-Sibai, Andreas Leefken, and Ulrich Renz. Local thickness and wave velocity measurement of wavy films with a chromatic confocal imaging method and a fluorescence intensity technique. *Experiments in Fluids*, 39(5):856–864, 2005.

[25] Flavia Viana, Raimundo Pardo, Rodolfo Ya´nez, Jos´e L. Trallero, and Daniel D. Joseph. Universal correlation for the rise velocity of long gas bubbles in round pipes. *International Journal of Multiphase Flow*, 29(4):609–635, 2003.

[26] A. D. K. Laird and Duncan Chisholm. Pressure and forces along cylindrical bubbles in a vertical tube. *Industrial & Engineering Chemistry*, 48(8):1361–1364, August 1956.

[27] Zhou G, Prosperetti A. Faster Taylor bubbles. J Fluid Mech. 2021;920:R2. doi:10.1017/jfm.2021.432. JFM Rapids.